9,10-Anthraquinone hinders β-aggregation: How does a small molecule interfere with Aβ-peptide amyloid fibrillation?

Marino Convertino,[1,2] Riccardo Pellarin,[1]* Marco Catto,[2] Angelo Carotti,[2] and Amedeo Caflisch[1]*

[1]Department of Biochemistry, University of Zurich, CH-8057 Zurich, Switzerland
[2]Dipartimento Farmaco-Chimico, Università degli Studi di Bari, I-70125 Bari, Italy

Received 19 November 2008; Revised 22 January 2009; Accepted 26 January 2009
DOI: 10.1002/pro.87
Published online 10 February 2009 proteinscience.org

Abstract: Amyloid aggregation is linked to a number of neurodegenerative syndromes, the most prevalent one being Alzheimer's disease. In this pathology, the β-amyloid peptides (Aβ) aggregate into oligomers, protofibrils, and fibrils and eventually into plaques, which constitute the characteristic hallmark of Alzheimer's disease. Several low-molecular-weight compounds able to impair the Aβ aggregation process have been recently discovered; yet, a detailed description of their interactions with oligomers and fibrils is hitherto missing. Here, molecular dynamics simulations are used to investigate the influence of two relatively similar tricyclic, planar compounds, that is, 9, 10-anthraquinone (AQ) and anthracene (AC), on the early phase of the aggregation of the Aβ heptapeptide segment $H_{14}QKLVFF_{20}$, the hydrophobic stretch that promotes the Aβ self-assembly. The simulations show that AQ interferes with β-sheet formation more than AC. In particular, AQ intercalates into the β-sheet because polar interactions between the compound and the peptide backbone destabilize the interstrand hydrogen bonds, thereby favoring disorder. The thioflavin T-binding assay indicates that AQ, but not AC, sensibly reduces the amount of aggregated $Aβ_{1–40}$ peptide. Taken together, the *in silico* and *in vitro* results provide evidence that structural perturbations by AQ can remarkably affect ordered oligomerization. Moreover, the simulations shed light at the atomic level on the interactions between AQ and Aβ oligomers, providing useful insights for the design of small-molecule inhibitors of aggregation with therapeutic potential in Alzheimer's disease.

Keywords: molecular dynamics; implicit solvent; Alzheimer's disease; 9,10-anthraquinone; amyloid; aggregation inhibition

Introduction

Fibrillar aggregation and plaques deposition of the β-amyloid peptide (Aβ) in the brain are common hallmarks of Alzheimer's disease. The Aβ peptide is a 39- to 43-residue segment generated by proteolysis of the amyloid precursor protein. Although little is known on the link between the aggregation mechanism and neurotoxicity,[1] experimental evidence indicates that soluble oligomers and fibrillar precursors of Aβ may be the neurotoxic species.[2]

Abbreviations: Aβ, β-amyloid peptide; AC, anthracene; AQ, 9,10-anthraquinone; MD, molecular dynamics; ThT, thioflavin T.

Grant sponsor: Ministry of University and Scientific Research, Rome, Italy (FIRB project); Grant number: RBAU01LSCE; Grant sponsor: Swiss National Competence Center in Neural Plasticity and Repair.

*Correspondence to: Riccardo Pellarin, or Amedeo Caflisch Department of Biochemistry, University of Zurich, Winterthurerstrasse 190, CH-8057 Zurich, Switzerland. E-mail: pellarin@bioc.uzh.ch or caflisch@bioc.uzh.ch

Several therapeutic strategies have been suggested for blocking different key-steps in the amyloid aggregation process, including the direct inhibition of the aggregation by using either peptides or small molecules.[3,4] N-methylated peptides[5,6] and L/D-polypeptides[7] were shown to block Aβ aggregation. Several nonpeptidic low-molecular-weight molecules were observed to reduce Aβ fibril formation and cytotoxicity,[8–10] in particular, scaffolds with aromatic or heteroaromatic rings have been identified as potent inhibitors of amyloid aggregation.[11] As an example, indole derivatives inhibited fibril formation of Aβ peptide[12] and lysozyme.[13] Rifampicin and *p*-benzoquinone reduced the toxicity of islet amyloid peptide aggregates[14] as well as inhibited amyloid fibril formation of hen egg-white lysozymes.[15] Anthraquinones were shown to be effective inhibitors of tau protein aggregation.[16] Notably, some small molecules active *in vitro* also showed beneficial activity against Alzheimer's disease in a mouse model.[17]

Molecular dynamics (MD) simulations have shed light on the very early events of amyloid aggregation.[18–28] These studies have focused on the driving forces governing the β assembly, emphasizing the role of aromatic packing,[19] hydrophobic forces[20,21,23,27] and electrostatic interactions.[20] The arrangement of peptides within oligomers and the process of reorganization have also been investigated by MD studies.[18,19,22,24,26] Moreover, the crucial role of amino acid sequence in determining the propensity to form aggregates has been studied in detail.[23,29] Recently, based on simulations of the inhibition of $A\beta_{16-22}$ fibrillation by a N-methylated peptide, it has been postulated that the inhibitor can bind to different sites of a preformed fibril, and thereby perturb it via different mechanisms.[30] Because of both poor oral absorption and low penetration through the blood-brain barrier, peptidic inhibitors have much smaller potential as drugs than small nonpeptidic compounds, although important exceptions based on nonnatural aminoacids exist.[31] The mechanism of inhibition of fibril formation by small compounds is however still obscure.

Here, we analyze the influence of two planar and tricyclic compounds on the early phase of ordered aggregation of a segment of the Aβ peptide that promotes oligomerization. Implicit solvent MD simulations are used to investigate the aggregation of three $A\beta_{14-20}$ (Ac-H_{14}QKLVFF$_{20}$-NHMe) terminally blocked heptapeptides in the presence and absence of AQ or AC. The $A\beta_{14-20}$ segment is chosen because it has a high β-aggregation propensity according to biophysical experiments,[32,33] as well as atomistic simulations[29,34] and a phenomenological equation based on physicochemical properties of the primary structure.[35] Notably, the MD simulations show that a small substitution in molecular structure (two carbonyl groups replacing two aromatic CH) results in significant differences in the ability to influence early aggregation. The simulation results are validated by the thioflavin T (ThT)-binding fluorimetric assay.

Results and Discussion

Properties of $A\beta_{14-20}$ aggregates with and without tricyclic compounds

During the simulation the three-peptide system explores many different configurations, including aggregated, disaggregated, β structures with a variety of registers, and other spatial arrangements. The P_2 order parameter (described in the Methods section) has been adopted to monitor the degree of orientational order within the oligomers: a value close to one corresponds to an ordered trimer, with either parallel or antiparallel β-sheet, while a value close to zero reflects a fully disordered system [Fig. 1(A)]. The frequency histograms of P_2 for the unperturbed and perturbed systems [Fig. 1(B)] display a prominent peak at $P_2 = 0.8$, and a shoulder for P_2 values lower than 0.5, which includes disordered aggregates and isolated peptides. The P_2 value for which the three distributions cross each other ($P_2^* = 0.665$) is chosen as the crossover value between ordered and disordered states. With this definition, the values of order-disorder ratio r can be calculated (Table I). AQ perturbs the oligomer order more than AC, suggesting that the quinonic moiety significantly contributes to the process of disorganization.

The frequency distribution of interpeptide interaction energies [Fig. 1(C)] shows two peaks. By visual inspection, and by comparing the energies with the average P_2 [circles in Fig. 1(C)], we could assign the oligomer structures relative to the different regions in the energy [see insets in Fig. 1(C)]. The peak at −80 kcal/mol and the peak at −40 kcal/mol correspond to a peptide placed in the centre and at the edge of an ordered trimer, respectively. From the plot it is evident that the simulations with AQ have more events with interaction energy close to zero, originating from unstructured peptides bound to the oligomeric or isolated monomers. This indicates that the system's order is perturbed by AQ, which is able to intercalate into the oligomer and influence its structure.

Binding mechanism

The interactions at the basis of the activity of AQ are the hydrogen bonds, the aromatic contacts and, moreover, the ability to establish a favorable interaction between the central electron-poor quinonic ring and the electron-rich peptidic carbonyls, which here is called as $\pi^+\delta^-$ interaction (see Figs. 2 and 3). A typical series of events leading to β structure disruption by AQ is described in Figure 2. Once approached the oligomer, AQ separates the ordered peptides by interacting with amide hydrogens (blue dashed lines). It then penetrates into the oligomer, interfacing the

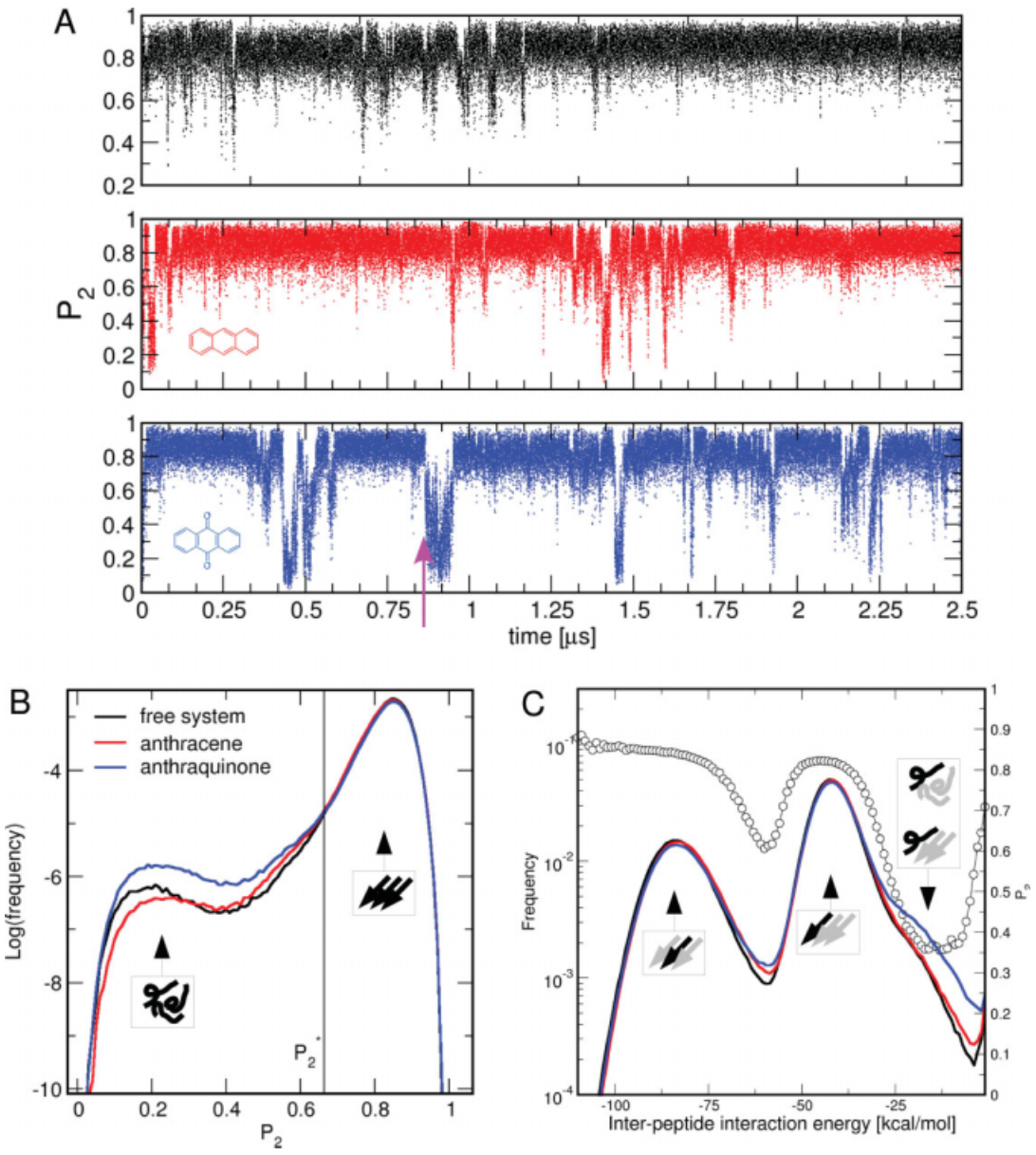

Figure 1. AQ hinders β-sheet formation more than AC. (A) Time series of the nematic order parameter P_2 for the free system (black), and in presence of AC (red) or AQ (blue). A similar behavior was observed in the other nine runs for each system. The magenta arrow indicates the temporal location of the snapshots shown in Figure 2. Molecular structures of AC and AQ are represented in the insets. (B) Distribution of the nematic order parameter P_2. Values of P_2 close to 0.2 and 0.8 correspond to disordered conformations and β-sheet structures, respectively. The three distributions cross each other at $P_2^* = 0.665$ (vertical solid line), which is the threshold value that separates the ordered from the disordered phase. (C) Interpeptide interaction energy distributions (solid lines, left *y*-axis; see Methods section) and average P_2 as a function of interaction energy (black circles, right *y*-axis). The two peaks of the energy distributions correspond to a peptide in the centre of an ordered oligomer (about −80 kcal/mol) and a peptide at the edge of an ordered oligomer (about −40 kcal/mol). The shoulder of the energy distribution at values of about −20 kcal/mol contains events with disordered or partially ordered oligomers. The P_2 values higher than 0.5 for interaction energy close to zero is due to the propensity of the isolated peptide for an extended conformation. The insets in (B) and (C) are schematic pictures of the oligomer conformations. [Color figure can be viewed in the online issue, which is available at www.interscience.wiley.com.]

carbonyl oxygens (red dashed lines). The β-sheet disruption is very rapid (less than 1 ns), which is in part a consequence of the low friction constant.

The distribution of backbone oxygens (see Fig. 3, top) shows the enrichment of coordinated carbonyl oxygens around the quinonic moieties of AQ with respect to the condensed aromatic rings of AC. Being able to coordinate two amide hydrogens, and two backbone carbonyl oxygens at the same time, the quinonic moiety plays a major role in the intercalation into the oligomer. In this way, AQ is able to sequestrate not only donors, but also acceptors of interchain

Table I. *Order-Disorder Ratio (r), Inhibition of Fibril Formation, and Number of Aromatic Contacts Between the Compounds and the Phenyl Rings of Phenylalanine*

System	r[a]	Activity[b] (%)	Aromatic contacts[c] (no. contacts per frame)
Unperturbed	10.2		
with AC	9.9	11	0.262
with AQ	6.7	33	0.242

[a] Ratio between order and disorder events sampled in the trajectories and estimated by Eq. (1).
[b] Inhibition of fibril formation measured by ThT fluorescence at a concentration of 30 μM $A\beta_{1-40}$ and 100 μM AC or AQ.
[c] Average number of aromatic contacts between the compounds and the phenyl ring of phenylalanine normalized by the total number of frames of simulations.

hydrogen bonds, which has three main consequences: (1) the disruption of the local intermolecular hydrogen bond geometry, (2) destabilization of the β-sheet structure, and (3) global disorganization of the oligomer, that is, reduction of the total order. On the other hand, AC is not able to interact with the peptides by hydrogen-bonds, or $\pi^+\delta^-$ interactions. Hydrophobic interactions alone are apparently not sufficient to perturb the ordered β architecture, as indicated by the similar values of r of the unperturbed and AC systems.

The number of aromatic contacts between the compounds and the phenyl rings of phenylalanine is reported in Table I. This interaction is slightly less frequent for AQ. This is due to the fact that, if compared with AC, AQ has also the ability to interact with peptide polar moieties, which are competitive with the hydrophobic ones. These results suggest that the aromatic interactions alone are not sufficient to drive the perturbation of $A\beta_{14-20}$ ordered oligomers, although they may favor the encounter of the tricyclic molecule with the peptides.

Experimental results on $A\beta_{1-40}$

The anti-aggregating activity of AC and AQ was determined in co-incubation experiments with $A\beta_{1-40}$ by monitoring maximal ThT emission intensity over the course of 21 days (see Methods section). As shown in Figure 4, the amyloid aggregation obeys the characteristic nucleation-dependent pattern, with three distinct phases: initial nucleation (lag phase), elongation, and

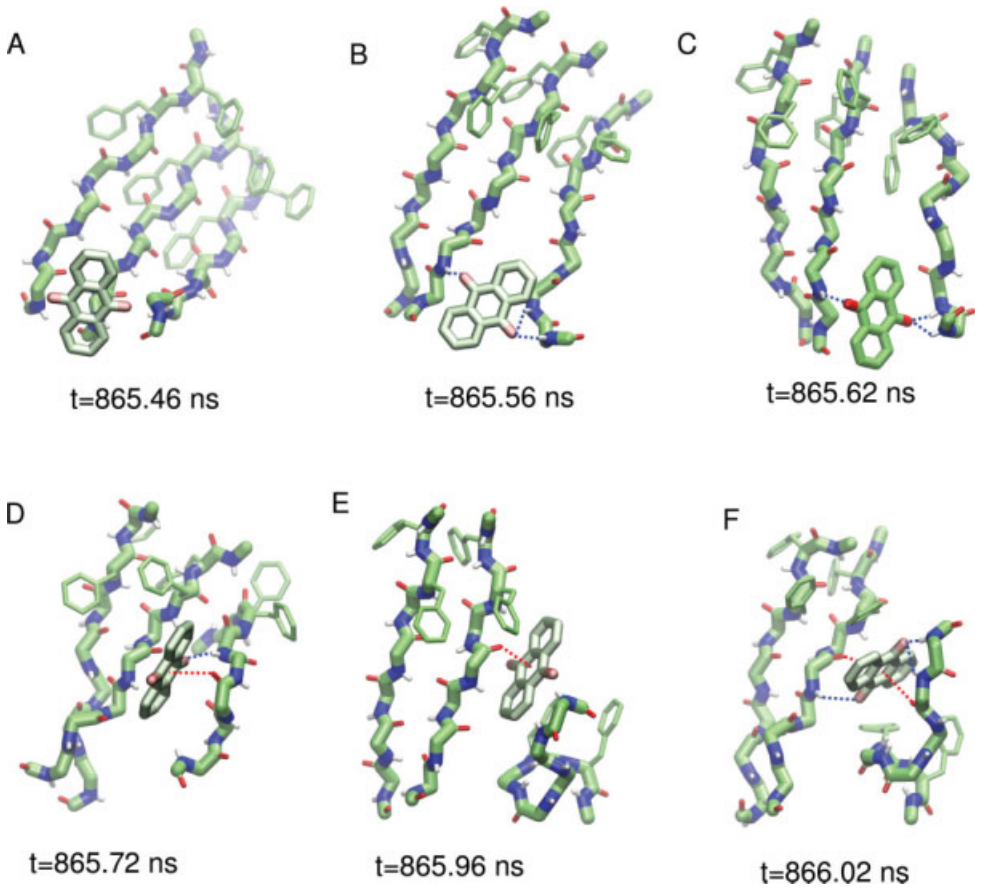

Figure 2. Atomistic details of β-sheet disruption by AQ. The times of the snapshots correspond to the time interval emphasized by an arrow in Figure 1(A). The quinonic moiety interacts with the peptide oligomer in a kind of "butter-knife" mechanism. AQ approaches the ordered oligomer (A) and starts to interact via hydrogen bond interactions (B and C, blue dashed lines). It subsequently intercalates into the ordered structure via hydrogen bonds and $\pi^+\delta^-$ interactions (D–F, red dashed line) and causes the disruption of the oligomer (F). [Color figure can be viewed in the online issue, which is available at www.interscience.wiley.com.]

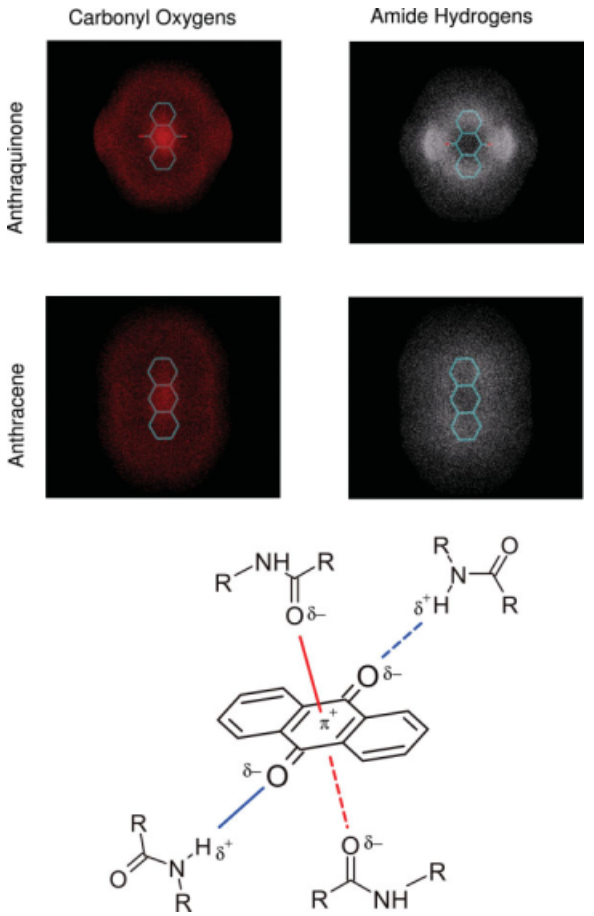

Figure 3. Interactions between backbone polar groups and AQ or AC. (Top) Positions of backbone carbonyl oxygens and amide hydrogens that are within 5 Å from any atom in AQ or AC are shown by dots to display the corresponding coordination. Denser clouds indicate a volume with higher coordination. (Bottom) $\pi^{+}\delta^{-}$ interaction scheme. Two electron-rich (δ^{-}) peptidic carbonyl oxygens interact with both faces of the electron-poor (π^{+}) AQ central ring.

equilibration. Under the present experimental conditions, the system reached its final equilibration phase after about 20 days. The shape of the curves presented in Figure 4 indicates that the final plateau is influenced by the presence of AQ and much less by AC. The ThT fluorescence emission intensity in the co-incubation with AQ (blue symbols) was nearly 33% lower than with the control peptide alone (black symbols). A significantly lower inhibitory effect, 11% decrease of ThT fluorescence emission intensity at the final plateau, was observed for AC (red symbols). The different inhibitory effects of AC and AQ are consistent with the MD simulation results (Table I). A quantitative agreement is not expected because of differences in the sequence (full-length Aβ in ThT assay versus seven-residue segment in MD), in relative mass concentrations, and temperature values (see Methods section).

The elongation rate marginally decreases in the presence of AQ, while the lag phase is not influenced at all by AQ or AC. Yamada and coworkers showed that nordihydroguaiaretic acid, curcumin, and rosmarinic acid, though reducing the amount of fibril at the equilibrium, did not extend the length of the lag phase in the formation of fibrillar Aβ, nor the time to proceed to equilibrium.[36] Recently, to explain the variable influence of compounds on $A\beta_{42}$ aggregation kinetics, a new mechanism of inhibition was suggested.[37] Compounds able to influence the elongation and the steady-state, but not the lag-phase, can prevent the self-assembly by blocking only the interstrand hydrogen-bond formation, in agreement with the AQ-binding mechanism discussed earlier, and not by stabilizing the nonamyloidogenic conformations of the polypeptide.

ThT measurements alone cannot unambiguously distinguish between inhibition of amyloid aggregation and competition of compounds with ThT binding. Meng *et al.*[38] showed that it is possible to determine whether an inhibitor is a false positive by adding the compound to a preincubated fibril sample and measuring ThT fluorescence thereafter. A fast decay (within few minutes) of the signal indicates that the compound is indeed competing with ThT. We measured the ThT fluorescence just after adding AQ and AC to two preincubated Aβ samples. Within few hours, we couldn't observe any signal decrease (data not shown), allowing us to exclude any direct competition between AC/AQ and ThT at the ThT-binding site.

Methods

Simulation protocol and analysis

The MD simulations were performed with the CHARMM program.[39] The peptide and compounds were modeled using the united atoms CHARMM

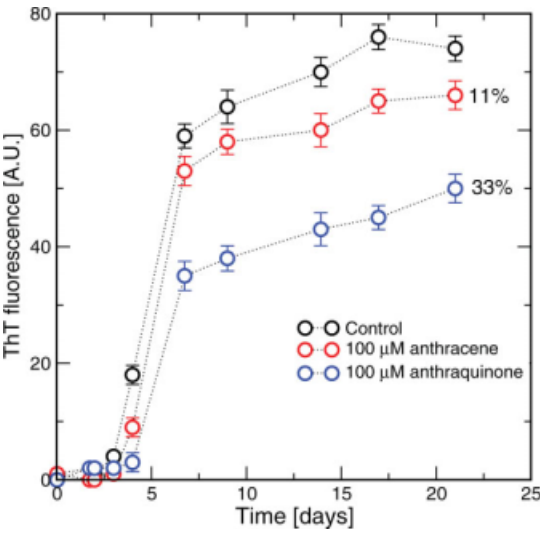

Figure 4. Time-dependent aggregation of $A\beta_{1-40}$ 30 μM, incubated in PBS (phosphate 10 mM, NaCl 100 mM, pH 7.4) at 25°C and monitored by ThT fluorescence. Error bars are standard deviations calculated from triplicate measures.

PARAM19 force field with its default truncation scheme for nonbonding interactions (cutoff of 7.5 Å). Hydration effects were accounted for by using SASA, a solvent-accessible surface based implicit model.[40] Partial charges for AQ were computed with the modified partial equalization of orbital electronegativity (MPEOE) algorithm.[41,42] To be consistent with the united atom model, charge summation of carbon atoms and their directly connected hydrogens was performed. The results were in agreement with the original CHARMM PARAM19 partial charges for phenylalanine, tryptophan and peptidic carbonyl. The difference in electronegativity between the oxygen atom in the peptidic moiety (partial charge: −0.55) and in the quinonic central ring (partial charge: −0.51) is due to the fact that the peptidic carbonyl is directly linked to a nitrogen, more electron-withdrawing with respect to the carbon atoms in the quinonic ring. There is a favorable interaction energy of −3.6 kcal/mol between *N*-methylacetamide and *p*-benzoquinone, computed at low dielectric conditions (i.e., distance depending dielectric function, without the SASA solvation contribution). This value is in agreement with the −3.9 kcal/mol value obtained by *ab initio* QM calculations.[43] To validate the parameterization of the bonding energy terms, two short MD simulations were performed for AQ and AC, using the SASA solvation model. Both molecules are stable, and the average bond distances and bond angles are comparable with the crystallographic data.[44]

The simulation box was prepared by introducing three monodispersed replicas of the same heptapeptide, with or without the presence of a single small molecule (AQ or AC). The concentration ratio peptide:compound of 3:1 is the minimal choice to have inhibitory effects and complex oligomeric structures. Note that the mass ratio peptide:compound is about 16 for the simulation and seven for the experiments (see ThT-Binding Assay section). To have the same mass ratio, one would have either to halve the compound concentration in the ThT assay, or to double the number of compounds in the simulation. In the first case the inhibition effect of AC would be undetectable. In the second case the compound-compound interactions would generate undesirable spurious effects, which is a disadvantage if one is interested in the oligomer–compound interaction mechanism. Simulations were carried out with periodic boundary conditions at fixed peptide concentration of 4.88 mM (the simulation box side was set to 98 Å), using Langevin integrator at low friction constant (0.1 ps^{-1}) and at the temperature of 330 K, which yields reversible aggregation within a reasonable computational time. Ten, 2.5 μs long, independent simulations were run for each system. A 2.5-μs run takes 3 weeks on a single AMD Opteron 252 CPU at 2.6 GHz.

Order parameters are useful quantities to monitor the structural transition within peptide oligomers.[25,29] In particular, the nematic order parameter P_2 allows to measure the amount of ordered β-structure in the system:

$$P_2 = \frac{1}{N}\sum_{i=1}^{N}\frac{3}{2}\left(\hat{\mathbf{z}}_i\cdot\hat{\mathbf{d}}\right)^2 - \frac{1}{2}$$

The unit vector $\hat{\mathbf{d}}$ that defines a preferential direction is the eigenvector of the order matrix that corresponds to the largest positive eigenvalue. The N molecular unit vectors $\hat{\mathbf{z}}_i$ are built joining the Cα atom of residue i to the Cα atom of residue $i + 2$ ($N = 3 \times 7$). The values of P_2 ranges from 0 to 1, which correspond to complete disorder and complete order, respectively. The complete order is achieved when all the unit vectors are parallel or antiparallel, while the disorder is obtained when none of unit vectors is parallel to any of the others.

P_2^* is a value of the order parameter chosen such that it separates the ordered from the disordered phase. Thus, the order-disorder ratio r is defined by the number of events where the system has a nematic order parameter lower than P_2^* (disorder) and greater that P_2^* (order):

$$r = \frac{n(P_2 > P_2^*)}{n(P_2 < P_2^*)} \quad (1)$$

Furthermore, the activity of the compounds is measured by calculating the interpeptide interaction energy, which is the CHARMM nonbond energy (van der Waals plus electrostatics) of a single peptide with the other two, without considering the compound molecule.

Aromatic contacts between the tricyclic compounds and the phenyl ring of Phe are calculated as follows. Given a trajectory frame, the centroids of the three rings of AC or AQ are calculated, together with the centroids of the six phenyl rings of Phe belonging to the three peptides. If any compound centroid is within 4 Å from any Phe centroid, then an aromatic contact is accounted. Note that more than one aromatic contact can be present at the same time, because the compounds have two sides available for the interfacing. The AC/AQ ratio of aromatic contacts is robust with respect to the choice of the cutoff up to 5 Å.

ThT-binding assay

The traditional spectrofluorimetric assay with ThT was chosen to assess the influence of the two tricyclic molecules, AQ and AC, on the kinetic of aggregation of $A\beta_{1-40}$. This technique easily enables to monitor the formation of β-sheet structures of aggregating peptides with ThT that leads to a marked increase of the fluorescence of ThT at defined wavelengths. Nevertheless, the β-sheet/ThT interaction is unselective and does not discriminate among oligomers, protofibrils, and

other transient species formed across the aggregation pathway.

The spectrofluorimetric assay was performed through the classical method of LeVine.[45] Briefly, ThT solution for fluorescence experiments was 25 μM in 25 mM phosphate buffer (pH 6.0). Quartz cuvette for aggregation tests contained $A\beta_{1-40}$ 30 μM control peptide (from AnaSpec, San José, CA) alone, or added either with AC or AQ 100 μM, in phosphate buffered saline (phosphate 10 mM, NaCl 100 mM, pH 7.4) containing 20% dimethyl sulphoxide to solubilize the test compounds. The concentration of compounds was chosen to have the highest yield of inhibition without precipitation effects. Samples were incubated at 25°C for 3 weeks. During this period, spectrofluorimetric readings were made in triplicate by dilution of 30 μL of sample in 470 μL of ThT solution at 25°C. Analyses were performed with a Perkin-Elmer LS 55 fluorimeter, in a 700-μL quartz cuvette, using FLWinLab software. Parameters were fixed as follows: excitation wavelength at 440 nm with 5-nm slit; emission at 485 nm with 10-nm slit; integration time 2 s. Plots of fluorescence emission intensity versus time (see Fig. 4) showed the typical sigmoidal curve of aggregation kinetics. Activities were calculated as percent of inhibition of free peptide aggregation after 3 weeks.

Conclusions

In previous works, the $A\beta_{14-20}$ heptapeptide was shown to have high aggregation propensity by biophysical experiments[32,33] and computational approaches,[34,35] suggesting a key role in the self-assembly of the full-length Aβ peptide. We have therefore hypothesized that the perturbation of the aggregation propensity of $A\beta_{14-20}$ can influence the assembly properties of the full-length Aβ sequence. Here, implicit solvent MD simulations have been used to investigate the effect of AQ and AC on the β-aggregation of three replicas of $A\beta_{14-20}$. The nematic order parameter P_2 was used to monitor the perturbation extent of β-aggregation.[34] Compared with AC, which is almost inert, AQ destabilizes the interstrand hydrogen bonds through favorable polar interactions with the backbone of the peptide. The quinonic moiety is able to tightly bind peptide backbone carbonyl oxygens and amide hydrogens through $\pi^+\delta^-$ interactions and hydrogen bonds, respectively, facilitating the intercalation of the molecule into the oligomer. The stability of the $\pi^+\delta^-$ interaction[46] has been previously documented in *ab initio* QM calculations,[43] the crystal packing of isocyanurate derivatives resolved by X-ray diffractometry,[47] and coordination of anions with electron-poor rings.[48,49]

Aromatic interactions have been shown to be determinant in the inhibition of fibril formation as well as the reduction of amyloid toxicity.[11] Our simulations reveal that such interactions favor the formation of the compound–oligomer complex, but are not sufficiently strong to significantly perturb the β-sheet formation of $A\beta_{14-20}$, as observed by comparing AC with AQ.

Perturbation of multimeric assembly is the basis for the activity of small compounds able to inhibit amyloid fibril formation. AQ only marginally affects the equilibrium properties of the unperturbed oligomeric system, that is, it slightly increases the disorderer events. Coarse grained simulations[50] have shown that even a small perturbation of the polypeptide free energy landscape, for example, a fraction of kcal/mol, dramatically influences the kinetics and the thermodynamics of the aggregation process. These simulation results could explain why a small perturbation produces the macroscopic decrease of amyloid aggregation observed *in vitro* in presence of inhibiting compounds. On the other hand, the slowing down or the inhibition of the ordered aggregation process, can multiply the alternative pathways for the aggregation,[51] increasing the chance to create other toxic species. For this reason, blocking the formation of oligomeric soluble species at their very early stages (note that the smallest oligomer, the Aβ dimer, has been recently reported to be synaptotoxic[52]) should be a viable strategy, providing that the accumulation of the Aβ monomer would not trigger any significant toxic effect.[53]

One of the main goals of the present work is the understanding of the interactions between tricyclic compounds and ordered oligomers. Knowledge of such interactions may suggest modifications of AQ for improving its antiaggregation activity. New functional groups potentially able to establish additional strong interactions with Aβ could be added to the quinonic scaffold to improve the strength of binding. Among them, positively charged aminic groups, such as those present in anthracyclinic and xantronic antitumor drugs, might be selected to engage in strong ionic interactions and hydrogen bonds with polar groups of Aβ. Indeed, some anthracyclines have shown excellent antifibrillogenic activity.[54] Moreover, pixantrone, an antitumor drug in phase III clinical trials for the treatment of relapsed or refractory indolent non-Hodgkin's lymphoma, showed activity and proved to selectively target soluble low oligomers of Aβ protein.[55] Another suggestion, inspired by the present simulation results, would be to link AQ to one or both termini of a recently discovered dipeptide inhibitor of Aβ oligomerization.[31] These experimental findings, together with the results obtained in the present study, provide useful insights for the design of new molecular entities targeting the early steps of formation of low oligomeric, toxic species.

Acknowledgments

The authors are grateful to F. Marchand and Dr. O. Nicolotti for interesting discussions and precious suggestions, Dr. R. Friedman for comments to the manuscript, and A. Widmer for providing the WitnotP program used

for visual analysis of the trajectories. The simulations were performed on the Matterhorn cluster of the University of Zurich and the support of C. Bolliger and A. Godknecht is gratefully acknowledged.

References

1. Lansbury PT, Lashuel HA (2006) A century-old debate on protein aggregation and neurodegeneration enters the clinic. Nature 443:774–779.
2. Haass C, Selkoe DJ (2007) Soluble protein oligomers in neurodegeneration: lessons from the Alzheimer's amyloid β-peptide. Nat Rev Mol Cell Biol 8:101–112.
3. Cohen FE, Kelly JW (2003) Therapeutic approaches to protein-misfolding diseases. Nature 426:905–909.
4. Necula M, Kayed R, Milton S, Glabe CG (2007) Small molecule inhibitors of aggregation indicate that amyloid β oligomerization and fibrillization pathways are independent and distinct. J Biol Chem 282:10311–10324.
5. Kokkoni N, Stott K, Amijee H, Mason JM, Doig AJ (2006) N-methylated peptide inhibitors of β-amyloid aggregation and toxicity. optimization of the inhibitor structure. Biochemistry 45:9906–9918.
6. Yan L-M, Velkova A, Tatarek-Nossol M, Andreetto E, Kapurniotu A (2007) IAPP mimic blocks Aβ cytotoxic self-assembly: cross-suppression of amyloid toxicity of Aβ and IAPP suggests a molecular link between Alzheimer's disease and type II diabetes. Angew Chem Int Ed Engl 46:1246–1252.
7. Ban T, Hoshino M, Takahashi S, Hamada D, Hasegawa K, Naiki H, Goto Y (2004) Direct observation of Aβ amyloid fibril growth and inhibition. J Mol Biol 344: 757–767.
8. Kanapathipillai M, Lentzen G, Sierks M, Park CB (2005) Ectoine and hydroxyectoine inhibit aggregation and neurotoxicity of Alzheimer's β-amyloid. FEBS Lett 579: 4775–4780.
9. Gervais F, Paquette J, Morissette C, Krzywkowski P, Yu M, Azzi M, Lacombe D, Kong X, Aman A, Laurin J, Szarek WA, Tremblay P (2007) Targeting soluble Aβ peptide with tramiprosate for the treatment of brain amyloidosis. Neurobiol Aging 28:537–547.
10. Mishra R, Bulic B, Sellin D, Jha S, Waldmann H, Winter R (2008) Small-molecule inhibitors of islet amyloid polypeptide fibril formation. Angew Chem Int Ed Engl 47: 4679–4682.
11. Porat Y, Mazor Y, Efrat S, Gazit E (2004) Inhibition of islet amyloid polypeptide fibril formation: a potential role for heteroaromatic interactions. Biochemistry 43: 14454–14462.
12. Cohen T, Frydman-Marom A, Rechter M, Gazit E (2006) Inhibition of amyloid fibril formation and cytotoxicity by hydroxyindole derivatives. Biochemistry 45:4727–4735.
13. Morshedi D, Rezaei-Ghaleh N, Ebrahim-Habibi A, Ahmadian S Nemat-Gorgani M (2007) Inhibition of amyloid fibrillation of lysozyme by indole derivatives-possible mechanism of action. FEBS J 274:6415–6425.
14. Tomiyama T, Kaneko H, Kataoka K, Asano S, Endo N (1997) Rifampicin inhibits the toxicity of pre-aggregated amyloid peptides by binding to peptide fibrils and preventing amyloid-cell interaction. Biochem J 322 (Part 3): 859–865.
15. Lieu VH, Wu JW, Wang SS-S, Wu C-H (2007) Inhibition of amyloid fibrillization of hen egg-white lysozymes by rifampicin and *p*-benzoquinone. Biotechnol Prog 23: 698–706.
16. Pickhardt M, Gazova Z, von Bergen M, Khlistunova I, Wang Y, Hascher A, Mandelkow E-M, Biernat J, Mandelkow E (2005) Anthraquinones inhibit tau aggregation and dissolve Alzheimer's paired helical filaments in vitro and in cells. J Biol Chem 280:3628–3635.
17. McLaurin J, Kierstead ME, Brown ME, Hawkes CA, Lambermon MHL, Phinney AL, Darabie AA, Cousins JE, French JE, Lan MF, Chen F, Wong SSN, Mount HTJ, Fraser PE, Westaway D, George-Hyslop PS (2006) Cyclohexanehexol inhibitors of Aβ aggregation prevent and reverse Alzheimer phenotype in a mouse model. Nat Med 12:801–808.
18. Ma B, Nussinov R (2002) Stabilities and conformations of Alzheimer's β-amyloid peptide oligomers (Aβ 16–22, Aβ 16–35, and Aβ 10–35): sequence effects. Proc Natl Acad Sci USA 99:14126–14131.
19. Gsponer J, Haberthür U, Caflisch A (2003) The role of side-chain interactions in the early steps of aggregation: Molecular dynamics simulations of an amyloid-forming peptide from the yeast prion Sup35. Proc Natl Acad Sci USA 100:5154–5159.
20. Klimov DK, Thirumalai D (2003) Dissecting the assembly of Aβ16–22 amyloid peptides into antiparallel β sheets. Structure 11:295–307.
21. Hwang W, Zhang S, Kamm RD, Karplus M (2004) Kinetic control of dimer structure formation in amyloid fibrillogenesis. Proc Natl Acad Sci USA 101:12916–12921.
22. Buchete N-V, Tycko R, Hummer G (2005) Molecular dynamics simulations of Alzheimer's β-amyloid protofilaments. J Mol Biol 353:804–821.
23. de la Paz ML, de Mori GMS, Serrano L, Colombo G (2005) Sequence dependence of amyloid fibril formation: insights from molecular dynamics simulations. J Mol Biol 349:583–596.
24. Melquiond A, Mousseau N, Derreumaux P (2006) Structures of soluble amyloid oligomers from computer simulations. Proteins 65:180–191.
25. Cecchini M, Rao F, Seeber M, Caflisch A (2004) Replica exchange molecular dynamics simulations of amyloid peptide aggregation. J Chem Phys 121:10748–10756.
26. Cheon M, Chang I, Mohanty S, Luheshi LM, Dobson CM, Vendruscolo M, Favrin G (2007) Structural reorganisation and potential toxicity of oligomeric species formed during the assembly of amyloid fibrils. PLoS Comput Biol 3:1727–1738.
27. Hills RD, Brooks CL (2007) Hydrophobic cooperativity as a mechanism for amyloid nucleation. J Mol Biol 368: 894–901.
28. Simone AD, Esposito L, Pedone C, Vitagliano L (2008) Insights into stability and toxicity of amyloid-like oligomers by replica exchange molecular dynamics analyses. Biophys J 95:1965–1973.
29. Cecchini M, Curcio R, Pappalardo M, Melki R, Caflisch A (2006) A molecular dynamics approach to the structural characterization of amyloid aggregation. J Mol Biol 357: 1306–1321.
30. Soto P, Griffin MA, Shea J-E (2007) New insights into the mechanism of Alzheimer amyloid-beta fibrillogenesis inhibition by N-methylated peptides. Biophys J 93: 3015–3025.
31. Frydman-Marom A, Rechter M, Bram Y, Shalev DE, Gazit E (2009) Cognitive performance recovery of Alzheimer's disease model mice by modulating early soluble amyloidal assemblies. Angew Chem Int Ed Engl 48:1981–1986.
32. Tjernberg LO, Näslund J, Lindqvist F, Johansson J, Karlström AR, Thyberg J, Terenius L, Nordstedt C (1996) Arrest of β-amyloid fibril formation by a pentapeptide ligand. J Biol Chem 271:8545–8548.
33. Williams AD, Portelius E, Kheterpal I, Tao Guo J, Cook KD, Xu Y, Wetzel R (2004) Mapping Aβ amyloid fibril secondary structure using scanning proline mutagenesis. J Mol Biol 335:833–842.

34. Caflisch A (2006) Computational models for the prediction of polypeptide aggregation propensity. Curr Opin Chem Biol 10:437–444.
35. Tartaglia GG, Cavalli A, Pellarin R, Caflisch A (2005) Prediction of aggregation rate and aggregation-prone segments in polypeptide sequences. Protein Sci 14:2723–2734.
36. Ono K, Hasegawa K, Naiki H, Yamada M (2004) Curcumin has potent anti-amyloidogenic affects for Alzheimer's β-amyloid fibrils in vitro. J Neurosci Res 75:742–750.
37. Bartolini M, Bertucci C, Bolognesi ML, Cavalli A, Melchiorre C, Andrisano V (2007) Insight into the kinetic of Amyloid β (1–42) peptide self-aggregation: elucidation of inhibitors' mechanism of action. Chem Biol Chem 8: 2152–2161.
38. Meng F, Marek P, Potter KJ, Verchere CB, Raleigh DP (2008) Rifampicin does not prevent amyloid fibril formation by human islet amyloid polypeptide but does inhibit fibril Thioflavin-T interactions: implications for mechanistic studies of β-cell death. Biochemistry 47:6016–6024.
39. Brooks BR, Bruccoleri RE, Olafson BD, States DJ, Swaminathan S, Karplus M (1983) CHARMM: A program for macromolecular energy, minimization, and dynamics calculations. J Comput Chem 4:187–217.
40. Ferrara P, Apostolakis J, Caflisch A (2002) Evaluation of a fast implicit solvent model for molecular dynamics simulations. Proteins: Struct Funct Bioinformat 46:24–33.
41. No K, Grant J, Scheraga H (1990) Determination of net atomic charges using a modified partial equalization of orbital electronegativity method. 1. Application to neutral molecules as models for polypeptides. J Phys Chem 94: 4732–4739.
42. No K, Grant J, Jhon M, Scheraga H (1990) Determination of net atomic charges using a modified partial equalization of orbital electronegativity method. 2. Application to ionic and aromatic molecules as models for polypeptides. J Phys Chem 94:4740–4746.
43. Li Y, Snyder L, Langley DR (2003) Electrostatic interaction of π-acidic amides with hydrogen-bond acceptors. Bioorganic & Medicinal Chemistry Letters 13:3261–3266.
44. Fu Y, Brock CP (1998) Temperature dependence of the rigid-body motion of Anthraquinone. Acta Cryst B 54: 308–315.
45. LeVine H, III. 1993. Thioflavine T interaction with synthetic Alzheimer's disease β-amyloid peptides: detection of amyloid aggregation in solution. Protein 2:404–410.
46. Meyer EA, Castellano RK, Diederich F (2003) Interactions with aromatic rings in chemical and biological recognition. Angew Chem Int Ed Engl 42:1210–1250.
47. Thalladi VR, Katz AK, Carrell HL, Nangia A, Desiraju GR (1998) Trimethyl isocyanurate and triethyl isocyanurate. Acta Crystallogr C 54 (Part 1):86–89.
48. Frontera A, Saczewski F, Gdaniec M, Dziemidowicz-Borys E, Kurland A, Deyà PM, Quiñonero D, Garau C (2005) Anion-π interactions in cyanuric acids: a combined crystallographic and computational study. Chemistry 11: 6560–6567.
49. Garau C, Frontera A, Quinonero D, Ballester P, Costa A, Deyà PM. (2004) Cation-π versus anion-π interactions: a comparative *ab initio* study based on energetic, electron charge density and aromatic features. Chem Phys Lett 392:85–89.
50. Pellarin R, Caflisch A (2006) Interpreting the aggregation kinetics of amyloid peptides. J Mol Biol 360:882–892.
51. Pellarin R, Guarnera E, Caflisch A (2007) Pathways and intermediates of amyloid fibril formation. J Mol Biol 374: 917–924.
52. Shankar GM, Li S, Mehta TH, Garcia-Munoz A, Shepardson NE, Smith I, Brett FM, Farrell MA, Rowan MJ, Lemere CA, Regan CM, Walsh DM, Sabatini BL, Selkoe DJ (2008) Amyloid-β protein dimers isolated directly from Alzheimer's brains impair synaptic plasticity and memory. Nat Med 14:837–842.
53. Brody DL, Magnoni S, Schwetye KE, Spinner ML, Esparza TJ, Stocchetti N, Zipfel GJ, Holtzman DM (2008) Amyloid-β dynamics correlate with neurological status in the injured human brain. Science 321: 1221–1224.
54. Bandiera T, Lansen J, Post C, Varasi M (1997) Inhibitors of Aβ peptide aggregation as potential anti-Alzheimer agents. Curr Med Chem 4:159–170.
55. Colombo R, Carotti A, Catto M, Racchi M, Lanni C, Verga L, Gabriele C, De Lorenzi E (in press) Capillary electrophoresis can identify small molecules that selectively target soluble oligomers of Aβ protein and display antifibrillogenic activity. Electrophoresis.